

NON-LOCAL EDDY DIFFUSIVITY MODEL FOR TURBULENT SCALAR FLUX

Fujihiro Hamba

Institute of Industrial Science
The University of Tokyo
Komaba, Meguro-ku Tokyo 153-8505, Japan
hamba@iis.u-tokyo.ac.jp

ABSTRACT

A non-local eddy diffusivity model for the turbulent scalar flux was recently proposed to improve the local model and was validated using direct numerical simulation (DNS) of homogeneous isotropic turbulence. Because the energy spectrum is used to express the non-local eddy diffusivity, the model is not sufficient to extend to inhomogeneous turbulence. In this study, to improve the non-local model, we use the scale-space energy density instead of the energy spectrum. A new model was proposed and validated using the DNS data. The temporal behaviour of the non-local eddy diffusivity was improved compared to the previous model. An attempt to apply the model to a turbulent channel flow was also made by incorporating an anisotropic effect.

INTRODUCTION

In the eddy diffusivity model, the turbulent scalar flux at a point is assumed to be proportional to the mean scalar gradient at the same point. However, this local approximation is not always valid for actual turbulent flows. A local gradient-transport model requires that the characteristic scale of the transport mechanism is small compared to the distance over which the mean gradient of the transported property changes appreciably. In turbulent flow, the length scale of turbulence is often as large as that of the mean-field variation.

Non-local expressions for the scalar flux were investigated theoretically using the Green's function. Using the direct interaction approximation, Kraichnan (1964) showed that the non-local eddy diffusivity can be approximated in terms of the averaged Green's function and velocity correlation. Moreover, using the Green's function for the scalar equation, Kraichnan (1987) derived an implicit exact non-local expression for the scalar flux. Hamba (1995) modified the Green's function to obtain an explicit exact expression for the scalar flux. The non-local eddy diffusivity was evaluated using the direct numerical simulation (DNS) of channel flow (Hamba 2004).

Non-local models have also been investigated by different approaches. For example, Mani and Park (2021) developed the macroscopic forcing method to reveal the differential operators associated with turbulence closures. Using this method Liu et al.

(2023) examined the non-local eddy diffusivity systematically and proposed reduced-order non-local models.

Recently, Hamba (2022b) examined the non-local expression for the scalar flux in detail using the DNS of homogeneous isotropic turbulence with an inhomogeneous mean scalar. A systematic model expression was proposed for the non-local eddy diffusivity, in which the two-point velocity correlation was expressed in terms of the energy spectrum. However, because the Fourier transform in homogeneous directions was used to define the energy spectrum, it is not clear whether the model can be applied to inhomogeneous turbulence.

In this study, we improve the non-local eddy diffusivity model by using the scale-space energy density developed by Hamba (2022a). We derive an expression for the two-point correlation using the scale-space energy density instead of the energy spectrum and propose a new model for the non-local eddy diffusivity (Hamba, 2023). The model was examined using the DNS data and compared to the previous model.

NON-LOCAL EXPRESSION FOR SCALAR FLUX

A non-local expression for the turbulent scalar flux $\langle u_i \theta \rangle$ can be written as

$$\langle u_i \theta \rangle(\mathbf{x}, t) = - \int d\mathbf{x}' \int_{-\infty}^t dt' \kappa_{NLij}(\mathbf{x}, t; \mathbf{x}', t') \frac{\partial}{\partial x'_j} \Theta(\mathbf{x}', t') \quad (1)$$

where u_i , θ , and Θ are the velocity fluctuation, the scalar fluctuation, and the mean scalar, respectively. Here, $\kappa_{NLij}(\mathbf{x}, t; \mathbf{x}', t')$ is the non-local eddy diffusivity, representing a non-local effect of the mean scalar gradient at (\mathbf{x}', t') on the scalar flux at (\mathbf{x}, t) . It is given by

$$\kappa_{NLij}(\mathbf{x}, t; \mathbf{x}', t') = \langle u_i(\mathbf{x}, t) g_j(\mathbf{x}, t; \mathbf{x}', t') \rangle \quad (2)$$

where $g_j(\mathbf{x}, t; \mathbf{x}', t')$ is the Green's function for the scalar fluctuation (Hamba 2022b).

We examined the DNS data of steady homogeneous isotropic turbulence with an inhomogeneous mean scalar to verify the non-local expression given by (1) (Hamba 2022b). Physical quantities were non-dimensionalized by the turbulence intensity $\langle u_i^2 \rangle^{1/2}$ and the length scale $L_x/2\pi$ (L_x is the domain size). In addition to the velocity field, we solved the transport

equation for the scalar fluctuation. A fixed one-dimensional profile of the mean scalar $\theta(y)$ was used as follows:

$$\frac{\partial \theta}{\partial y} = \begin{cases} \cos y, & \text{case 1} \\ \cos 2y + (1 + \cos 4y)/4, & \text{case 2} \end{cases} \quad (3)$$

Because the velocity field is statistically steady and homogeneous in the x and z directions, the non-local expression given by (1) can be rewritten as

$$\langle u_y \theta \rangle_{NL}(y) = - \int_{-\infty}^{\infty} dy' \kappa_{NLyy}(y; y') \frac{\partial \theta}{\partial y'} \quad (4)$$

where

$$\kappa_{NLyy}(y; y') = \int_{-\infty}^{\infty} dx' \int_{-\infty}^{\infty} dz' \int_{-\infty}^t dt' \kappa_{NLyy}(\mathbf{x}, t; \mathbf{x}', t') \quad (5)$$

Figure 1 shows the profiles of the scalar fluxes as functions of y for the two cases. The profiles of $\langle u_y \theta \rangle_{NL}$ given by (4) agree with the DNS values for both cases. This agreement verifies the non-local expression for the scalar flux given by (1). In contrast, the profiles of $\langle u_y \theta \rangle_L$ for the local model overpredicted the DNS values.

NON-LOCAL DIFFUSIVITY BASED ON SCALE-SPACE ENERGY DENSITY

We consider an expression for the non-local eddy diffusivity for isotropic velocity field

$$\kappa_{NLij}(\mathbf{r}, \tau) = \langle u_i(\mathbf{x}, t) g_j(\mathbf{x}, t; \mathbf{x}', t') \rangle = \kappa_{NL}(r, \tau) \delta_{ij} \quad (6)$$

which is a function of $\mathbf{r} (= \mathbf{x} - \mathbf{x}')$ and $\tau (= t - t')$ for homogeneous and steady turbulence. We investigate the non-local eddy diffusivity $\kappa_{NL}(r, \tau)$ and its time integral $\kappa_{NL}(r)$ given by

$$\kappa_{NL}(r) = \int_0^{\infty} d\tau \kappa_{NL}(r, \tau) \quad (7)$$

We model the non-local eddy diffusivity in terms of the two-point velocity correlation $Q_{ii}(\mathbf{r}) (= \langle u_i(\mathbf{x}, t) u_i(\mathbf{x}', t) \rangle)$ as follows:

$$\kappa_{NL}(r, \tau) = G(r, \tau) Q(r) \quad (8)$$

where $Q(r) = Q_{ii}(\mathbf{r})/3$. The time-dependent part $G(r, \tau)$ appearing in (8), which corresponds to the mean Green's function for the scalar fluctuation, was given by

$$G(r, \tau) = \frac{1}{(4\pi)^{3/2} (C_{\omega G} u_0 \tau)^3} \exp\left[-\frac{r^2}{4(C_{\omega G} u_0 \tau)^2}\right] \quad (9)$$

where $u_0 = \langle u_i^2 \rangle^{1/2} = (2K)^{1/2}$ and $C_{\omega G}$ is a model constant. In Hamba (2022b), the two-point correlation $Q(r)$ was expressed in terms of the Kolmogorov energy spectrum. In this work, we used the scale-space energy density developed by Hamba (2022a).

We introduce two filtered velocities. The first filtered velocity $\bar{u}_i(\mathbf{x}, s)$ is based on a Gaussian filter. It is defined as

$$\bar{u}_i(\mathbf{x}, s) = \int d\mathbf{x}' \bar{G}(\mathbf{x} - \mathbf{x}', s) u_i(\mathbf{x}') \quad (10)$$

where $\bar{G}(\mathbf{x}, s)$ is the filter function given by

$$\bar{G}(\mathbf{x}, s) = \frac{1}{(2\pi s)^{3/2}} \exp\left(-\frac{\mathbf{x}^2}{2s}\right) \quad (11)$$

The filtered velocity $\bar{u}_i(\mathbf{x}, s)$ represents the velocity with a scale greater than s . By differentiating $\bar{u}_i(\mathbf{x}, s)$ with respect to s , we can obtain a filtered velocity with a scale equal to s :

$$\hat{u}_i(\mathbf{x}, s) \equiv -\frac{\partial}{\partial s} \bar{u}_i(\mathbf{x}, s) = \int d\mathbf{x}' \hat{G}(\mathbf{x} - \mathbf{x}', s) u_i(\mathbf{x}') \quad (12)$$

The original velocity $u_i(\mathbf{x})$ can be written as

$$u_i(\mathbf{x}) = \int_0^{\infty} ds \hat{u}_i(\mathbf{x}, s) \quad (13)$$

Next, we consider the two-point correlation of filtered velocities with the same scale as follows:

$$\bar{Q}_{ii}(\mathbf{x}_1, \mathbf{x}_2, s) = \langle \bar{u}_i(\mathbf{x}_1, s) \bar{u}_i(\mathbf{x}_2, s) \rangle \quad (14)$$

Another correlation can be defined as

$$\hat{Q}_{ii}(\mathbf{x}_1, \mathbf{x}_2, s) \equiv -\frac{\partial}{\partial s} \bar{Q}_{ii}(\mathbf{x}_1, \mathbf{x}_2, s) \quad (15)$$

Using the second correlation we can decompose the original velocity correlation into modes in the scale space as follows:

$$Q_{ii}(\mathbf{r}) = \int_0^{\infty} ds \hat{Q}_{ii}(\mathbf{r}, s) \quad (16)$$

In the case of $\mathbf{r} = \mathbf{0}$, the turbulent kinetic energy can be decomposed as

$$\langle u_i^2 \rangle = \int_0^{\infty} ds \hat{Q}_{ii}(s) \quad (17)$$

where $\hat{Q}_{ii}(s) (= \hat{Q}_{ii}(\mathbf{0}, s))$ is the energy density in the scale space. Figure 2 shows profiles of the pre-multiplied energy density $s\hat{Q}_{ii}(s)$ as functions of s . The DNS value was plotted in black line. Symbols represent the locations of six scales at which two-point correlations are plotted in Figs 3 and 4. We propose a simple expression for the energy density as follows:

$$\hat{Q}_{ii}(s) = \begin{cases} v^{-1} \varepsilon, & s < s_d \\ C_s \varepsilon^{2/3} s^{-2/3}, & s_d \leq s \leq s_c \\ C_s \varepsilon^{2/3} s_c^{11/6} s^{-5/2}, & s > s_c \end{cases} \quad (18)$$

where $s_d (= C_s^{3/2} v^{3/2} \varepsilon^{-1/2})$ and $s_c [= (6/11)^3 C_s^{-3} K^3 \varepsilon^{-2} (1 + C_s^{3/2} v^{1/2} K^{-1} \varepsilon^{1/2})^3]$ are the scales of the dissipation and energy-containing ranges, respectively. The profile of $s\hat{Q}_{ii}(s)$ given by (18) with $C_s = 1.9$ reasonably agrees with the DNS data.

For the two-point correlation we propose the following model

$$\hat{Q}_{ii}(\mathbf{r}, s) = \hat{Q}_{ii}(s) \exp(-r^2/4s) \quad (19)$$

Figure 3 shows the DNS profiles of $\hat{Q}_{ii}(\mathbf{r}, s)$ for six scales varying from $s = 0.00094$ to 0.96 . As s increases, the peak value decreases and the profile becomes wider. Figure 4 shows the profiles of $\hat{Q}_{ii}(\mathbf{r}, s)$ normalised by $\hat{Q}_{ii}(s)$ as functions of $r/s^{1/2}$ for six scales. Despite the self-similarity not holding very well, the function approximately reproduces overall profiles decaying as $r/s^{1/2}$ increases.

Now, we obtained a new model expression for $\kappa_{NL}(r, \tau)$ given by (8) with (9), (18) and (19). The model constants were set to $C_s = 1.3$ and $C_{\omega G} = 0.46$. Despite (18) with $C_s = 1.9$ giving a good profile in Fig. 2, it leads to a too narrow profile of $\kappa_{NLyy}(y - y')$ (not shown here). The optimised value was $C_s = 1.3$. Figure 5 shows the profiles of $r^2 \kappa_{NL}(r)$. As r increases, the profiles of models decay slightly slowly compared to the DNS value, and the profile of the new model is better than that of the previous model based on the energy spectrum.

Figure 6 shows the profiles of $\kappa_{NL}(r, \tau)$ at $\tau = 0.2$ and 0.4 . As time difference τ increases, the peak value at $r = 0$ decays rapidly and the width increases gradually. This means that the spatial region in which the mean scalar gradient non-locally affects the scalar flux is very narrow for small τ and becomes wider as τ increases. The profiles of the previous model show small values whereas those of the new model agree well with the DNS value. The new model is more adequate for modelling the temporal behaviour of $\kappa_{NL}(r, \tau)$.

As an attempt to extend the model to inhomogeneous turbulence, we show a preliminary result obtained from the DNS of a turbulent channel flow at $Re_{\tau} = 180$. The velocity fluctuations are statistically homogeneous in the streamwise (x) and spanwise (z) directions and inhomogeneous in the wall-

normal (y) direction. Figure 7 shows two-dimensional contour plots of the non-local eddy diffusivity given by

$$\kappa_{NLyy}(x-x', y, y', \tau) = \int dz \kappa_{NLyy}(x-x', y, y', z-z', \tau) \quad (20)$$

directly evaluated by the DNS in the $x-y$ plane for $y' = -0.7$ ($y'^+ = 54$) at $\tau = 0.025$ and 0.05 . As τ increased, the contours were shifted downstream by the mean velocity and their peak values decayed.

A model for the non-local eddy diffusivity can be written as

$$\kappa_{NLyy}(x-x', y, y', z-z', \tau) = G(x-x', y, y', z-z', \tau) Q_{yy}(x-x', y, y', z-z') \quad (21)$$

Using the Reynolds stress $R_{ij}(= \langle u_i u_j \rangle)$, the two-point correlation is expressed as

$$Q_{yy}(x-x', y, y', z-z') = \frac{R_{yy}(y')}{R_{ii}(y')} Q_{jj}(r_x, r_y, r_z) \quad (22)$$

where $r_x = x - x' - U_x(y')\tau$, $r_y = y - y'$ and $r_z = z - z'$. Here $Q_{jj}(\mathbf{r})$ is given by (16). To incorporate an anisotropic effect, we modified the time-dependent part G as

$$G(x-x', y, y', z-z', \tau) = \frac{1}{(12\pi C_{\omega G}^2 \tau^2)^{3/2} \det(\mathbf{R})^{1/2}} \exp\left(-\frac{R_{ij}^{-1} r_i r_j}{12 C_{\omega G}^2 \tau^2}\right) \quad (23)$$

Figure 8 shows contour plots of the nonlocal eddy diffusivity given by (21) with (22) and (23). The contours were shifted downstream adequately by the mean velocity. Because of the turbulence anisotropy, the contours were elongated in the streamwise direction and slightly tilted towards the bottom wall. The overall agreement with the DNS value suggests that the present model can be extended to inhomogeneous turbulence.

CONCLUSIONS

A new model for the non-local eddy diffusivity was proposed using the turbulent energy density in the scale space based on the filtered velocities. Instead of the energy spectrum, we used the scale-space energy density to express the two-point velocity correlation involved in the model. The new model was validated using the DNS data of homogeneous isotropic turbulence with an inhomogeneous mean scalar. It was shown that the temporal behaviour of the non-local eddy diffusivity was improved compared to the previous model. By incorporating an anisotropic effect, the non-local eddy diffusivity was evaluated for a turbulent channel flow. It is expected that the new model can also be applied to wall-bounded turbulence.

REFERENCES

- Hamba, F., 1995, "An analysis of nonlocal scalar transport in the convective boundary layer using the Green's function", *J. Atmos. Sci.*, Vol. 52, pp. 1084-1095.
- Hamba, F., 2004, "Nonlocal expression for scalar flux in turbulent shear flow", *Phys. Fluids.*, Vol. 16, pp. 1493-1508.
- Hamba, F., 2022a, "Scale-space energy density for inhomogeneous turbulence based on filtered velocities", *J. Fluid Mech.*, Vol. 931, A34.
- Hamba, F., 2022b, "Analysis and modelling of non-local eddy diffusivity for turbulent scalar flux", *J. Fluid Mech.*, Vol. 950, A38.
- Hamba, F., 2023, "Non-local eddy diffusivity model based on turbulent energy density in scale space", *J. Fluid Mech.*, Vol. 977, A11.

Kraichnan, R. H., 1964, "Direct-interaction approximation for shear and thermally driven turbulence", *Phys. Fluids*, Vol. 7, pp. 1048-1062.

Kraichnan, R. H., 1987, "Eddy viscosity and diffusivity: exact formulas and approximations", *Complex Systems*, Vol. 1, pp. 805-820.

Liu, J., Williams, H. H., and Mani, A., 2023, "Systematic approach for modeling a nonlocal eddy diffusivity", *Phys. Rev. Fluids*, Vol. 8, 124501.

Mani, A., and Park, D., 2021, "Macroscopic forcing method: a tool for turbulence modeling and analysis of closures", *Phys. Rev. Fluids*, Vol. 6, 054607.

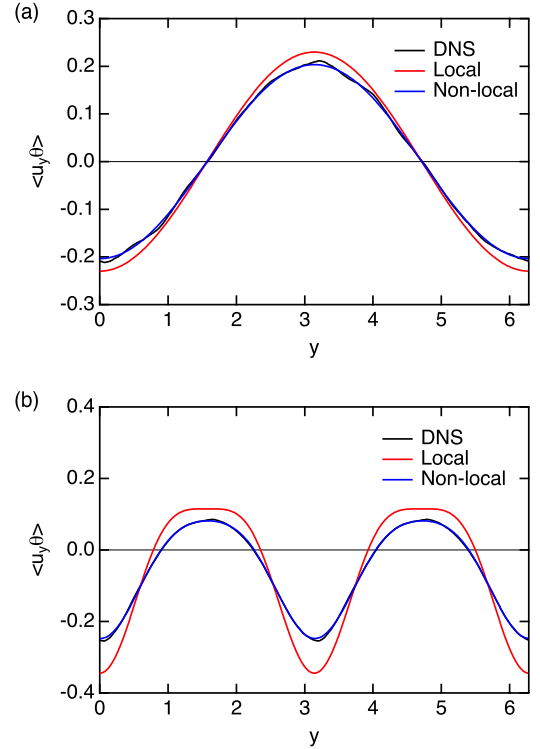


Figure 1. Profiles of the scalar fluxes as functions of y for (a) case 1 and (b) case 2.

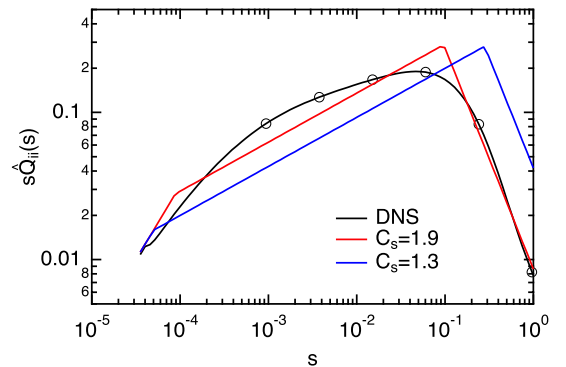


Figure 2. Profiles of the pre-multiplied energy density $s \hat{Q}_{ii}(s)$ as functions of s for DNS and (18) with $C_s = 1.9$ and 1.3 .

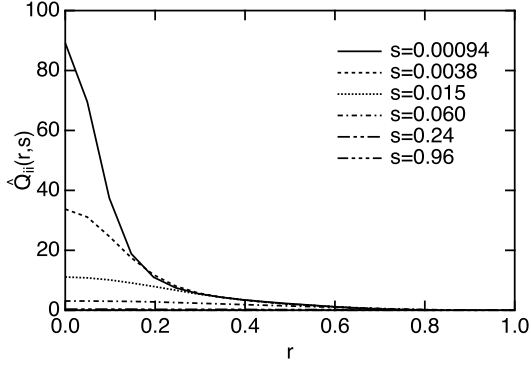


Figure 3. Profiles of the two-point correlation $\hat{Q}_{ii}(\mathbf{r}, s)$ as a function of r at six scales in the scale space.

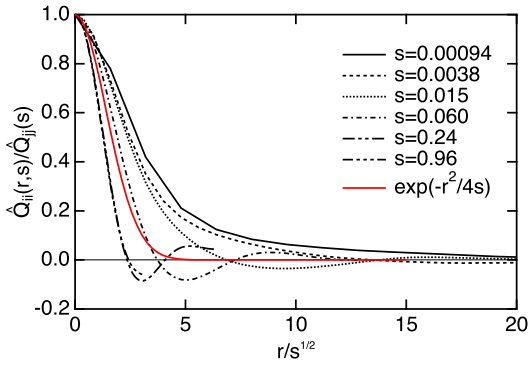


Figure 4. Profiles of the two-point correlation $\hat{Q}_{ii}(\mathbf{r}, s)$ normalised by $\hat{Q}_{ii}(s)$ as a function of $r/s^{1/2}$ at six scales in the scale space.

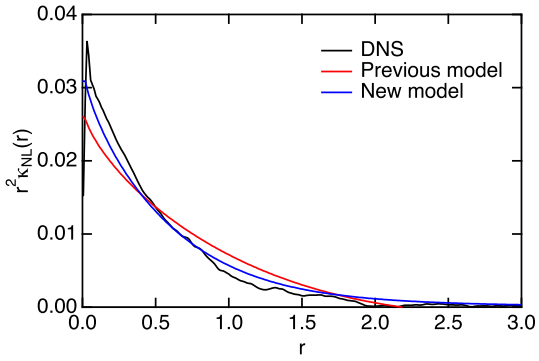


Figure 5. Profiles of $r^2 \kappa_{NL}(r)$ as functions of r for DNS and models.

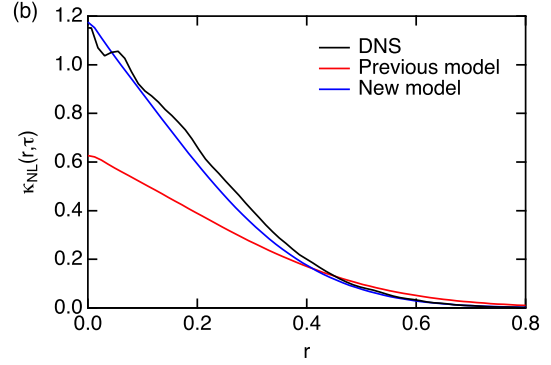
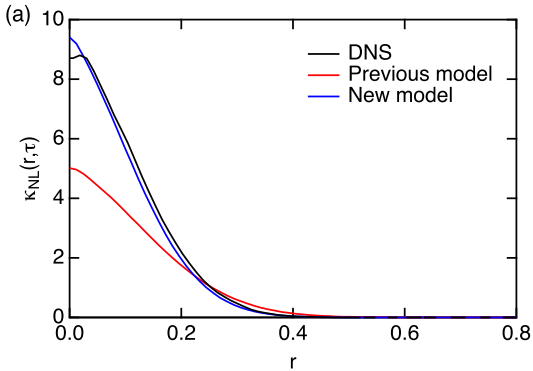


Figure 6. Profiles $\kappa_{NL}(r, \tau)$ as functions of r for DNS and models at (a) $\tau = 0.2$ and (b) $\tau = 0.4$.

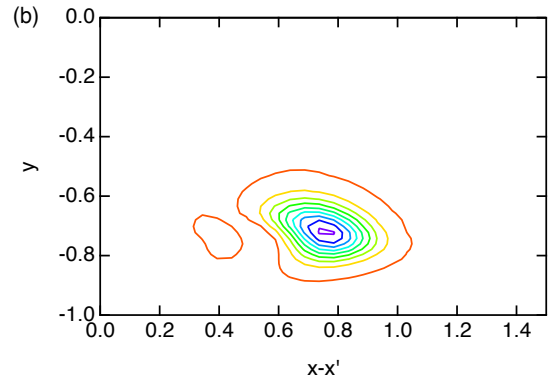
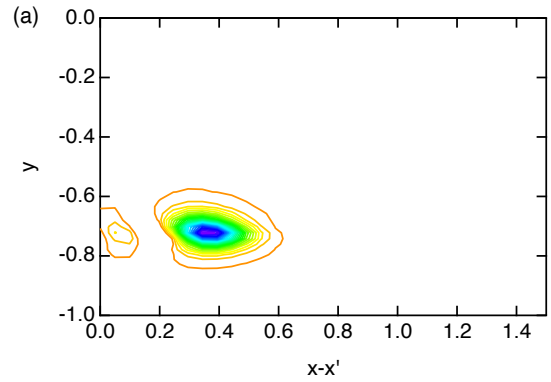
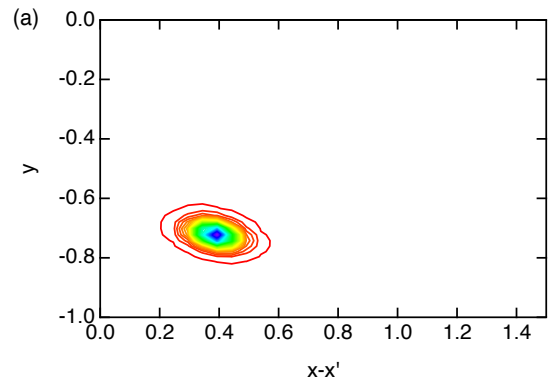


Figure 7. Contour plots of $\kappa_{NLyy}(x - x', y, y', \tau)$ for channel flow obtained from the DNS in the $x - y$ plane for $y' = -0.7$ at (a) $\tau = 0.025$ and (b) $\tau = 0.05$. The contour values range from 0.2 with an increment of 1.6.



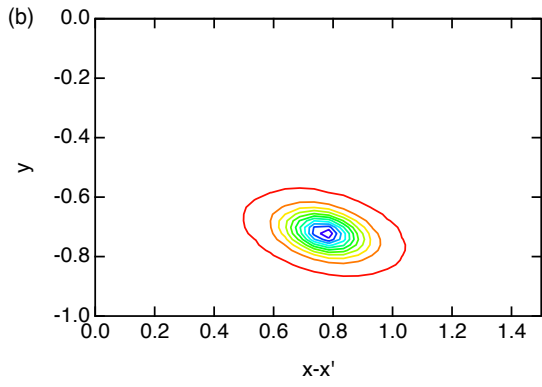


Figure 8. Contour plots of $\kappa_{NLYY}(x-x', y, y', \tau)$ for channel flow obtained from the model in the $x-y$ plane for $y' = -0.7$ at (a) $\tau = 0.025$ and (b) $\tau = 0.05$. The contour values range from 0.2 with an increment of 1.6.